Prod. Eng. Res. Devel. (2010) 4:477–482
DOI 10.1007/s11740-010-0240-7

PRODUCTION PROCESS

Numerical analysis of the process chain for the production of PM components with integrated information storage

Bernd-Arno Behrens · Edin Gastan · Najmeh Vahed · Fabian Lange

Received: 9 March 2010 / Accepted: 9 June 2010 / Published online: 22 June 2010

Abstract The powder metallurgical production offers a number of advantages compared to other manufacturing technologies. A few examples are the high level of material utilization, the production of net-shape parts and an extensive amount of alloying options. This paper describes the production process to integrate component relevant information in the component to increase its functional range. The analysis of the production process is done by means of numerical simulation. Therefore, the process chain, consisting of die pressing and sintering, is modeled based on a finite-element-analysis.

Keywords Production process · Powder metallurgy (PM) · Finite-element-analysis (FEA)

1 Introduction

The integration of a component with its related information offers a big flexibility in components application. Data stored inside the component are always available and can not be lost during the lifecycle. In addition, the components are marked in terms of protection against plagiarism.

In this paper, the FE based analysis of an approach to storing information inside PM components is presented. The focal point of this analysis is the local density distribution in a cylindrical specimen that is marked with an embedded foreign particle. The results are used to get an indication whether the component is weakened by the marking or not.

The production process in general as well as the method for information readout is given in the second chapter. The next chapters deal with the numerical simulation of the process chain which consists of the die pressing process (chapter three) and the sintering process (chapter four). The conclusions are presented in chapter five.

2 Production process and information readout

For the production of a component with integrated information, the classic powder-metallurgic production process is slightly modified. The powder pressing process is presented in Fig. 1.

The die is filled with a part of the powder. After smoothing of the powder surface, foreign particles are positioned on the powder. This can be done manually with a template or automatically by means of a positioning device (e.g. a 3-axial system consisting of linear bearings with a gripper). After filling in the remaining powder, parent powder and foreign particles are pressed into a compact—the so-called green compact. This green compact is then sintered in order to give it its strength.

The storage principle is based on the systematical placement of foreign particles in the powder. The particles are positioned as a binary-coded matrix. In Fig. 2, this is shown exemplarily for a 4×4 matrix.

Each position in the matrix represents a power of two (2^0, 2^1, 2^2, etc.), and for every foreign particle, the respective power of two is added to the number stored in the component (for example, workpiece identification number or batch number). The maximum storage capacity can be increased with the size of the applied matrix.

B.-A. Behrens · E. Gastan · N. Vahed · F. Lange (✉)
Institute of Metal Forming and Metal-Forming Machines (IFUM), Leibniz Universität Hannover, An der Universität 2, 30823 Garbsen, Germany
e-mail: lange@ifum.uni-hannover.de
URL: www.ifum.uni-hannover.de

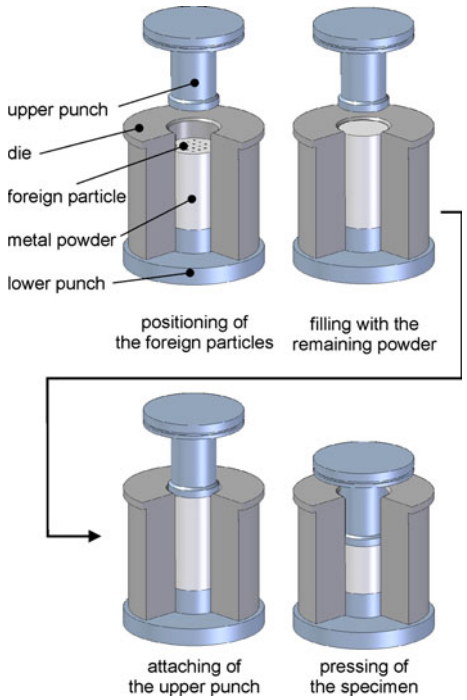

Fig. 1 Powder pressing process

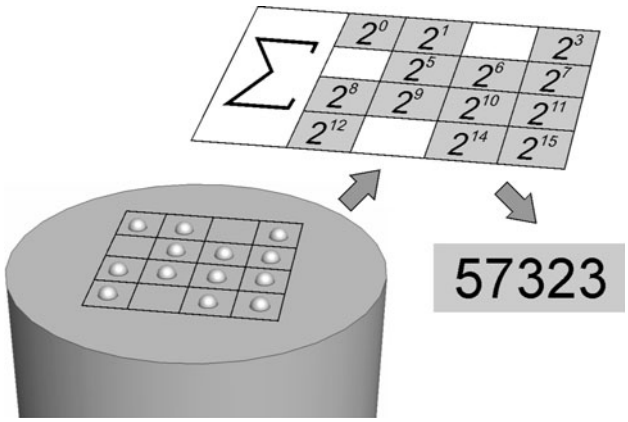

Fig. 2 Storage principle

The readout of information from the component can be done contactless and nondestructively via *x*-rays, for example. This principle is based on the different physical properties of parent powder and foreign particles. Different combinations of parent powder and foreign particles were investigated, for example magnesium/steel, aluminum/steel or iron/ceramic (first mentioned is the parent powder, second mentioned the foreign particles). In Fig. 3, a radiograph of a toothed belt disk made of iron powder with a 4 × 4 matrix of ceramic particles is shown.

The differences in density of the material combination can be clearly detected. This result was also obtained for the other material combinations mentioned earlier [1, 2].

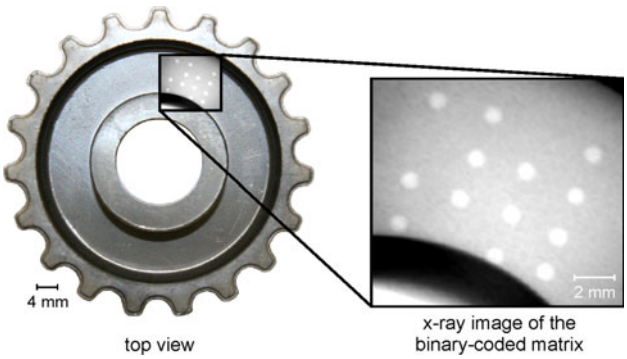

Fig. 3 Data readout of a toothed belt disk with stored information

3 Pressing process

In the first step of the numerical analysis, the pressing process of the component is analyzed. Subsequently, process modeling is described (chapter 3.1) followed by the numerical results of the analysis (chapter 3.2).

3.1 Process modeling

The powder material is described by the Drucker-Prager cap model which has its origin in soil mechanics [3]. The model describes the material as an elasto-plastic, compressible continuum. Figure 4 shows the model in the plane of hydrostatic pressure p and the von Mises equivalent stress q.

The elastic region is bordered on both sides. On the left side, the elastic area is limited by the failure line. This is characterized by the shear strength d and the angle of inner friction β. If the failure line is reached, the strength decreases with the risk of a crack initiation. On the right side, the elastic area is bordered by an elliptically shaped cap. If a stress state reaches the cap, the material is compressed and this leads to an increase in strength [4]. The equations describing the failure line (F_V) and the elliptically shaped cap (F_K) are:

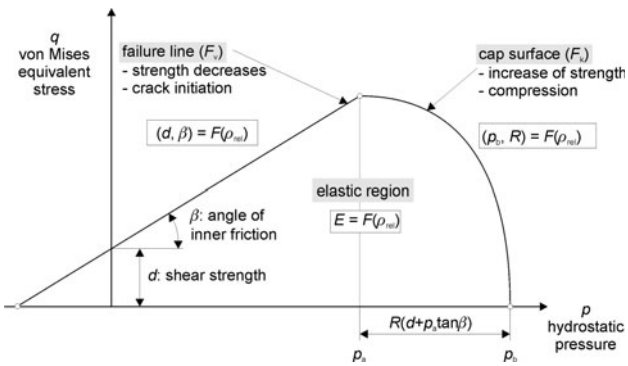

Fig. 4 Drucker-Prager cap model

$$F_V = q - p\tan\beta - d = 0 \quad (1)$$

$$F_K = \sqrt{(p-p_a)^2+(Rq)^2} - R(d + p_a\tan\beta) = 0. \quad (2)$$

The FEA software used, Abaqus/Standard, includes a formulation of the Drucker-Prager cap model, independent of the porosity, which is described by the relative density (ratio of powder volume to the total volume). To increase the accuracy of the simulation, the dependency of the material model on the relative density is introduced by user-defined subroutines.

As light weight materials are becoming more and more important, aluminum was chosen as powder material. The data needed for the analyzed aluminum powder is taken from [5, 6]. The elastic modulus of the powder is also formulated as a function of the relative density.

For the material of the foreign particles steel was chosen, because steel particles can be easily detected in aluminium powder and they are available at low cost. The stresses on the steel particles are relatively low compared to the yield stress, therefore they are considered as elastic bodies. For the modelling a Young's modulus of $E = 210000$ N/mm^2 and a Poisson's ratio of $\nu = 0.3$ were used. The use of a constant friction coefficient is not suitable to describe the friction of powder-metallurgic forming processes [7, 8]. For a more realistic modeling of the friction, the friction model of Coulomb is extended by the dependency on the relative density [9, 10].

3.2 Results of the simulation

The focus of the investigation by numerical simulation is on the local density distribution in the component. During sintering, mass transport occurs from high-density to low-density areas. Therefore, the density distribution in the green compact has a considerable effect on the component's distortion due to sintering.

The investigations on cylindrical specimens provide a basis for statements about the inserted particles' influence on the density distribution. Within the framework of this analysis, only a single embedded foreign particle was considered. Preliminary calculations [11] have shown that there is only a slight interaction between two particles with a given diameter/distance ratio like given in Fig. 3. Due to the simple geometry, the number of influence factors is limited. The cylindrical specimens (diameter 20 mm) are made of aluminum by means of two-sided pressing (initial powder height 45 mm with an initial relative density of 0.55, green compact height 27 mm). The foreign particle has a diameter of 1 mm. The models used are 2D axi-symmetric. In Fig. 5, the results for a test specimen with and without an embedded foreign particle are shown for comparison.

As a measure for the density distribution in the component, the relative density is shown:

$$\rho_{\text{rel}} = \frac{\text{volume of the powder particles}}{\text{total volume}}. \quad (3)$$

Due to friction between powder and die, the resulting density gradient is symmetrical to the horizontal midplane. The friction counteracts the powder's movement at the die wall, and thus the densification of the powder is impeded there. This effect can be observed for both kinds of specimens. Due to the influence of wall friction, foreign particles should not be placed near the die wall. Otherwise, it can not be assured that all particles are located in the same plane after the pressing process.

The foreign particle has only a localized effect on the density distribution. The range of influence covers approximately twice the sphere diameter. The powder movement around the foreign particle is, analogously to that at the die wall, impeded by friction. This leads to the presented distribution of the relative density with a minimum in the sphere's equatorial plane.

In order to estimate the friction influence, comparative computations neglecting the friction are done. Figure 6 shows the distribution of the relative density around the foreign particle with a density-dependent friction law and for frictionless modeling.

On the left side of Fig. 6, the results with a density-dependent friction law are shown, while on the right side the friction between powder and foreign particle was

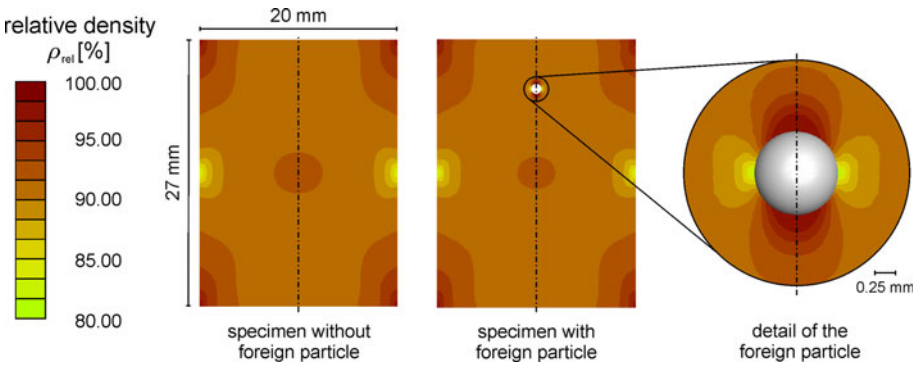

Fig. 5 Comparison of specimens with and without foreign particles

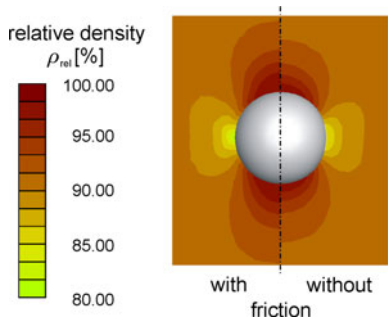

Fig. 6 Comparison of the relative density with and without friction

neglected. As can be seen, the areas of the highest and the lowest density correspond. However, while the distributions correspond qualitatively, the foreign particle's range of influence is—as expected—larger with existing friction. The distributions of the relative density show that, even with ideal absence of friction, a density gradient surrounding the sphere arises nonetheless.

4 Sintering process

In the second step of the numerical analysis, the sintering process of the component is analyzed. Subsequently, the process modeling is described (chapter 4.1) followed by the numerical results of the analysis (chapter 4.2).

4.1 Process modeling

The mechanical behavior during the sintering phase is described by a linear viscous law. For an isotropic material, the general form is given by

$$\dot{\underline{\varepsilon}}^{vp} = \frac{\underline{\sigma}'}{2G} + \underline{1} \cdot \frac{tr(\underline{\sigma}) - 3\sigma_s}{9K} \tag{4}$$

where $\dot{\underline{\varepsilon}}^{vp}$ is the strain rate tensor, $\underline{\sigma}'$ is the deviatoric part of the stress tensor, $tr(\underline{\sigma})$ is the trace of the stress tensor, $\underline{1}$ is the unit tensor, G and K are the shear and the bulk viscosity, and σ_s is the sintering stress. Both G, K, and σ_s depend on the current relative density, on the temperature and on the transport mechanism that supports densification [12].

For this analysis, a model for solid state sintering is used [13, 14] with grain boundary diffusion as the dominant transport mechanism. This model gives:

$$G = \frac{\sqrt{3} k_B T (1-\omega)^3 d_{fac}^3}{48 \Omega D_K} \tag{5}$$

$$K = \frac{4G}{3} \left(\frac{1-\rho_{ref}}{1-\rho_{rel}} \right)^{(m+1)/(m+5/3)} \tag{6}$$

$$\sigma_s = \sigma_{s,ref} \left(\frac{1-\rho_{ref}}{1-\rho_{rel}} \right)^{1/(3m+5)}. \tag{7}$$

Here Ω is the atomic volume, D_K is the grain boundary diffusion coefficient, k is the Boltzmann's constant, T is the absolute temperature, d is the grain facet diameter, ρ_{rel} is a reference density, $\sigma_{s,ref}$ is the sintering stress at the reference density, and ω is the voided area fraction of the grain boundary.

4.2 Results of the simulation

In order to estimate the effects of foreign particles on the sintering process, a 2D axial-symmetric model of a cylindrical sample was taken as a basis along with a single introduced foreign particle. Hereby, effects resulting from complex geometry can be detached. The sintering model uses values of relative density and net-geometry as input parameters, which had been determined within the scope of the simulation of the pressing process. Therefore, mapping of the density values is not necessary.

Because of the locally limited effect of the foreign particles on the density distribution, only a portion of the sample shall be examined. The definition of the examined area is exhibited in Fig. 7.

Focusing on the analysis, the question presents itself in what form or degree the density gradient around the foreign particle changes during the sintering process. The characteristic

$$\Delta\rho_{rel,\,max-min} = \rho_{rel,\,max} - \rho_{rel,\,min} \tag{8}$$

is to be defined in order to describe the size of the density gradient. It can be calculated from the highest relative density $\rho_{rel,\,max}$ and the smallest relative density $\rho_{rel,\,min}$ around the foreign particle. The following characteristics have been defined to analyze the difference of the density minimum/maximum and the density of the particle's surrounding $\rho_{rel,\,surr.}$:

$$\Delta\rho_{rel,\,max-surr.} = \rho_{rel,\,max} - \rho_{rel,\,surr.} \tag{9}$$

$$\Delta\rho_{rel,\,surr.-min} = \rho_{rel,\,surr.} - \rho_{rel,\,min}. \tag{10}$$

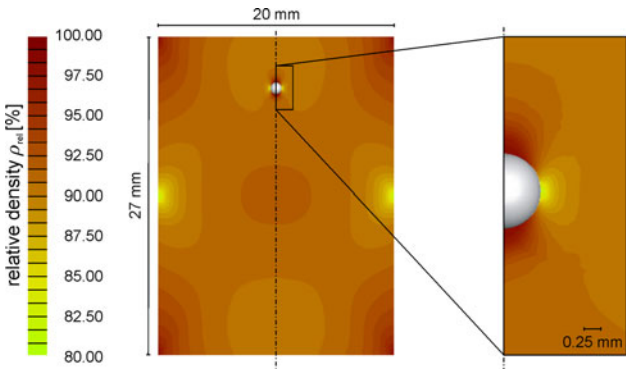

Fig. 7 Definition of the examined sample section (relative density at the beginning of the sintering process)

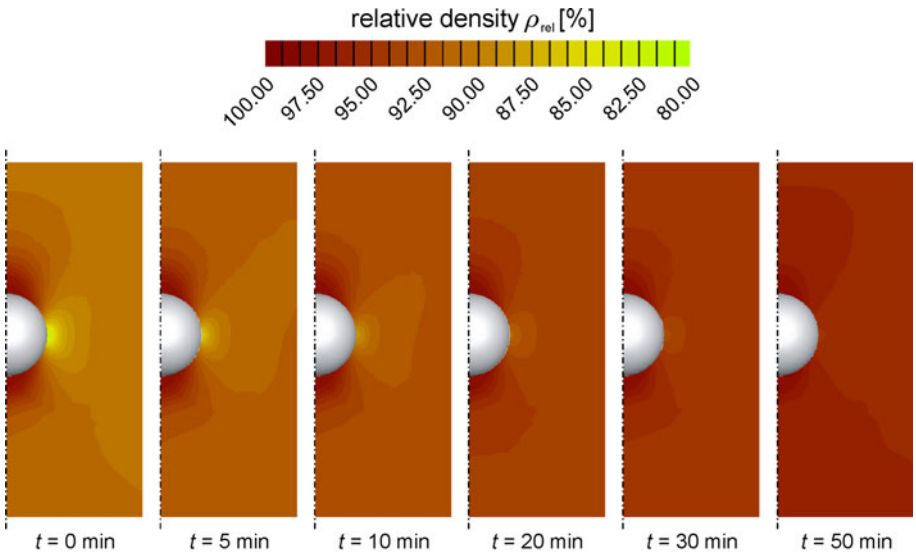

Fig. 8 Time-dependent changes of the relative density during the sintering process (sintering temperature 600°C)

Table 1 Density difference between minimum and maximum of the relative density around a foreign particle and the relative density of the surrounding

t (min)	$\rho_{rel,\ max}$ (%)	$\rho_{rel,\ max}$ (%)	$\Delta\rho_{rel,\ max-min}$ (%)	$\rho_{rel,\ surr.}$ (%)	$\Delta\rho_{rel,\ max-surr.}$ (%)	$\Delta\rho_{rel,\ surr.-min}$ (%)
0	97.58	81.54	16.04	90.5	7.1	9.0
5	97.66	85.64	12.02	92.0	5.7	6.4
10	97.74	88.17	9.57	92.5	5.2	4.3
20	97.88	91.12	6.76	94.0	3.9	2.9
30	97.98	92.80	5.18	94.5	3.5	1.7
50	98.16	94.69	3.47	96.0	2.2	1.3

The following states of the sintering process (sintering temperature 600°C) relate to the times indicated in Fig. 8. It can be determined that the density gradient decreases quickly around the foreign particle during the course of the sintering process. This can be supported quantitatively by means of the characteristic $\Delta\rho_{rel,\ max-min}$, of which the result values have been summarized in Table 1 for the examined times.

The minimal value of the relative density quickly increases while the maximal value of the relative density does so only slowly. This leads to the fact that after a sintering time of 50 min for the characteristic $\Delta\rho_{rel,\ max-min}$, a mere value of approximately 3.5% is exhibited.

As shown in Fig. 8, for the time $t = 50$ min, practically no density gradient can be ascertained upon the equatorial plane towards the end of the sintering process, as opposed to the surrounding area. The value for $\Delta\rho_{rel,\ surr.-min}$ or, more exactly, the difference of the surrounding density and minimal density on the foreign particle surface, comes to a mere 1.3% (compared with Table 1). On the basis of this value, it is to be presumed that only a slight weakening of the solidity of the component takes place. A small density increase remains above the foreign particle as opposed to the surrounding area. Towards the end of the sintering process for $\Delta\rho_{rel,\ max-surr.}$, a value of 2.2% is to be ascertained.

5 Conclusions

Within this paper, a procedure was presented that allows storage of information in a powder-metallurgically manufactured component by means of inserted foreign particles. The stored information is secure against subsequent manipulation and thus contributes to the protection against plagiarism.

By a numerical simulation of the process chain (die pressing and sintering), the influence of the foreign particles on the density distribution of the surrounding powder was estimated. As a result of the pressing process, a density gradient was created. Above and below the particles, the density is increased and in the equatorial plane, the density is decreased in comparison to the surrounding powder material. The sintering process reduces areas of low density significantly but has only a minor influence on areas of high density.

The presented results can be used for assumptions on how an embedded particle influences the relative density of

pm components. For the given cylindrical specimen, there seems to be no weakening of the component. This hypothesis was supported by experimental compression tests with cylindrical specimens with and without embedded foreign particles [15].

Acknowledgments The results presented in this paper were obtained within the framework of the Collaborative Research Center 653 "Gentelligent Components in their Lifecycle" [16] in the subproject "Sintering gentelligent parts from metal powder". The authors would like to thank the German Research Foundation for its financial support of this project. The authors would also thank the Institute of Materials Science (IW) for producing the x-ray image shown in this paper.

References

1. Behrens B-A, Lange F, Gastan E (2008) Experimental and numerical analysis of marking approach for sintered light alloy components. Powder Met 51/3:277–282
2. Behrens B-A, Bach Fr-W, Reimche W, Gastan E, Lange F, Mroz G (2008) Verfahren zur Einbringung und Wiedergabe von Daten in Sinterbauteilen. Metall 62/5:298–301
3. Drucker DC, Gibson RE, Henkel DJ (1957) Soil mechanics and work-hardening theories of plasticity. Trans Am Soc Civil Eng 122:338–346
4. Kraft T (2003) Optimizing press tool shapes by numerical simulation of compaction and sintering—application to a hard metal cutting insert. Model Simul Mater Sci Eng 11:381–400
5. Behrens B-A, Bouguecha A, Hanini K (2004) Ermittlung der Versagenslinie von Aluminiumpulver für das Drucker-Prager-Kappenmodell. wt Werkstattstechnik online 94/10:508–511
6. Behrens B-A, Bouguecha A, Hanini K (2004) Beschreibung des Verfestigungsverhaltens von Aluminiumpulver im Drucker-Prager-Kappenmodell. UTF Sci 5/2:1–4
7. Wikman B, Larsson R, Oldenburg M (2000) Wall friction coefficient estimation through modelling of powder die pressing experiment. Powder Metal 43/2:132–138
8. Cameron IM, Gethin DT, Tweed JH (2002) Friction measurement in powder die compaction by shear plate technique. Powder Metal 45/4:34–353
9. Behrens B-A, Bouguecha A, Hanini K (2004) Ermittlung dichteabhängiger Reibkoeffizienten für das Pressen von Aluminiumpulver. UTF Sci 5/4:1–3
10. Hanini K (2006) Simulationsgestützte Algorithmen für die automatisierte Auslegung von Pulverformgebungsprozessen. PhD-thesis, Universität Hannover
11. Lange F, Behrens B-A, Gastan E, Helms G (2008) Manufacturing of powder-metallurgical components with integrated information. In: Proceedings 12th International Conference Metal Forming 2008, Krakow (Poland), pp 486–492
12. Sun D-Z, Riedel H (1995) Prediction of shape distortions of hard metal parts by numerical simulation of pressing and sintering, in simulation of materials processing: theory, methods and applications. In: Proceedings of the Fifth International Conference on Numerical Methods in Industrial Forming Processes, Ithaca, New York (USA), pp 881–886
13. Riedel H (1990) A constitutive model for the finite-element simulation of sintering—distortions and stresses, in ceramic powder science III. In: Proceedings of the Third International Conference on Ceramic Powder Processing, San Diego, pp 619–630
14. Riedel H, Sun D-Z (1992) Simulation of die pressing and sintering of powder metals, hard metals and ceramics, in simulation of materials processing: theory, methods and applications. In: Proceedings of the Fourth International Conference on Numerical Methods in Industrial Forming Processes, Valbonne (France), pp 883–886
15. Behrens B-A, Lange F, Gastan E (2008) Plagiatschutz sicherheitsrelevanter Sinterbauteile—Verfahrensprinzip und Betrachtung erreichbarer Bauteilfestigkeiten und Risssicherheiten, wt Werkstattstechnik online, 98/10:880–884
16. Denkena B, Henning H, Lorenzen L-E (2010) Genetics and intelligence—new approaches in production engineering. Prod Eng 4/1:65–73